COMPACT STARS, HEAVY ION COLLISIONS AND POSSIBLE LESSONS FOR QCD AT FINITE DENSITIES*

Thomas Klähn[a], David Blaschke[a,b], R. Łastowiecki[a]

[a]Institute for Theoretical Physics, University of Wrocław, Poland
[b]Bogoliubov Laboratory for Theoretical Physics, JINR Dubna, Russia

(Received January 2, 2012)

Large neutron star masses as the recently measured $1.97 \pm 0.04\,M_\odot$ for PSR J1614-2230 provide a valuable lower limit on the stiffness of the equation of state of dense, nuclear and quark matter. Complementary, the analysis of the elliptic flow in heavy ion collisions suggests an upper limit on the EoS stiffness. We illustrate how this dichotomy permits to constrain parameters of effective EoS models which otherwise could not be derived unambiguously from first principles.

DOI:10.5506/APhysPolBSupp.5.757
PACS numbers: 04.40.Dg, 12.38.Mh, 26.60.+c, 97.60.Jd

1. Introduction

Neutron stars (NS) which outrange the domain of 'typical' NS masses (very roughly between 1.2 and $1.6\,M_\odot$, see Fig. 1 in [1] for an overview) have been considered to provide a serious constraint on the stiffness of the equation of state (EoS) [2] but treated rather cautiously due to the fact that in the rare cases of very massive observed NS either the accuracy of the measurement has been worryingly low or/and the measurement itself raised doubts within the community [3]. It seems that this situation has changed after a mass of $M = 1.97 \pm 0.04\,M_\odot$ has been reported for PSR J1614-2230 with an unprecedented accuracy in this high mass regime [4] and without perceivable objections from expert groups involved in this field. This observation of a two solar mass NS provides a very direct constraint on the minimum stiffness of the EoS of cold and dense matter and, therefore, promises new insights regarding our understanding in particular of *the nature of particle interactions at finite densities*. Implications have been discussed shortly after the measurement became public [1].

* Talk presented at HIC for FAIR Workshop and XXVIII Max Born Symposium "Three Days on Quarkyonic Island", Wrocław, Poland, May 19–21, 2011.

As an example (which deserves more attention than can be granted in this article) for the importance of this result, it is worth to mention the problem of strangeness for the hadronic EoS. Even though we are rather interested in the possible existence of a quark matter (QM) core in NS one cannot exclude the possibility that before the according critical density can be reached, the mass-density threshold for hyperons is passed and the EoS has to soften due to the appearance of these additional degrees of freedom. Due to this softening, the maximum mass of a corresponding NS can decrease drastically in comparison to the plain EoS with only neutron and proton degrees of freedom and is, therefore, not unlikely to contradict the high NS mass constraint. The problem can be avoided by accounting for repulsive vector interaction terms which are a specific feature of relativistic approaches to EoS. This has been shown, *e.g.*, in a generalized nonlinear Walecka-type model [5, 6] and a quark-meson-coupling model [7, 8]. Similarly, it turns out that vector interaction terms are of crucial importance if aiming at the description of high mass NS with QM cores [9]. It is an interesting finding that merely by the observation of a two solar mass NS the vector interaction can be identified as an inevitable channel if approaching a microscopical description of both, dense hyperon and QM.

Besides a two solar mass constraint limiting the 'softness' of the EoS, we suggested several other constraints from NS observations and the analysis of heavy ion collisions which have to be fulfilled *simultaneously* by a viable state-of-the-art EoS [2]. In detail, the scheme suggests that a viable EoS should:

- reproduce the most massive observed neutron star,
- avoid the direct URCA (DU) cooling problem,
- result in neutron stars within the predicted mass-radius domains of 4U 0614+09 (deduced from quasiperiodic brightness oscillations) and RX J1856-3754 (deduced from the objects thermal emission),
- explain the gravitational mass and total baryon number of pulsar PSR J0737-3039(B) with at most 1% deviation from the baryon number predicted for this particular object, and
- not contradict flow and kaon production data of heavy-ion collisions.

At the time of publication of Ref. [2], the most massive NS has been PSR J0751+1807 with $M \sim 2.1\,M_\odot$, a result which later has been withdrawn [10]. We reasoned that, in particular, the flow constraint is an extremely useful constraint. In contrast to the two solar mass constraint it limits the EoS such, that it cannot exceed the upper limits on the pressure (as a function of density) in symmetric matter as obtained from the analysis of the elliptic flow of iso-symmetric matter in HIC [11]. This gives two complementing phenomenological constraints on the EoS stiffness, an upper (flow) and

a lower (two solar mass constraint) limit, which both considered together significantly reduce the possible shape of the pressure density relation, *viz.*, the EoS at super saturation densities. In previous work, we took advantage of this insight and adjusted otherwise not well determined coupling constants of a Nambu–Jona-Lasinio (NJL) type model. Details about these models framework is found in the original work formulated before the invention of the quark model of elementary particles [12, 13] and a number of review articles [14, 15, 16, 17, 18] applying it to elucidate the role of dynamical chiral symmetry breaking for hadron structure and its restoration in dense quark matter. Our resulting hybrid, nuclear-quark matter EoS, is in agreement with both of these before mentioned constraints and shows a better overall performance than the originally underlying nuclear EoS based on the Dirac–Bruckner Hartree–Fock (DBHF) approach [9], which will be shortly summarized later in this paper. At this time we had to scan a small parameter range only in order to obtain this result. However, the question how well the QM model EoS is constrained, *viz.* which other sets of coupling constants would reproduce a phenomenologically sound EoS, has been left open in [9]. The reporting of PSR J1614's high mass has triggered this kind of more systematic studies for Bag-like QM EoS within a purely phenomenological model for the QM equation of state consisting simply of a power series expansion in the quark chemical potential μ including 4th and 2nd order terms [19, 20]. The 4th-order term is thought to mimic the influence of strong interactions on the ideal gas expression for the quark pressure, while the 2nd order term is a measure for the competing effects of a finite strange quark mass and a possible diquark condensate in deconfined matter [21]. It is worth to notice that a μ^4-term is not necessarily the leading order term in a μ-expansion of the pressure, as has been shown for a simple, semi-analytic model based on Dyson–Schwinger techniques at finite densities [22]. We would like to mention a very promising, recent development in modeling quark matter in the nonperturbative, low-energy domain of QCD which is relevant for the QCD phase diagram and compact star phenomenology. This concerns nonlocal, separable interaction models with either covariant or instantaneous formfactors [23, 24, 25] and their application to compact stars [26, 27] generalizing the local current–current coupling of the NJL model. In particular, the rank-2 separable models which allow a simultaneous description of the dynamical quark mass function $m(p)$ and the wave function renormalization $Z(p)$ of the quark propagator in accordance with lattice QCD data [28, 29, 30, 31] shall allow to greatly reduce ambiguities of the parametrization of quark models discussed in these proceedings. For the time being, however, the nonlocal models need to be further improved to address diquark condensation and asymmetric matter before they can be used to study compact star constraints.

In this paper, we will illustrate in a systematic, 'whole-range' scan of an NJL model EoS for QM how strongly a two-solar NS mass measurement constrains the strength of available (vector and diquark) coupling strength parameters and what implications can be derived for the investigation of HIC, *viz.* the EoS of iso-spin symmetric matter. Section 2 gives a summary of the applied QM EoS, Sec. 3 discusses the result of our analysis, Sec. 4 will provide conclusions and a brief outlook concerning further interesting questions.

2. Hybrid matter EoS based on a NJL model

In order to obtain a QM equation of state, we employ a three-flavor color superconducting NJL model with selfconsistently determined quark masses and diquark gaps [32, 33, 34]. In addition to a typical scalar interaction term, we account for a repulsive vector interaction term which stiffens the EoS with increasing interaction strength and results in sufficiently high NS masses (details are found in [9] and references therein). The attractive scalar diquark channels are responsible for the formation of diquark condensates and color superconducting phases in the system. As we discussed before, it moreover lowers the transition density to a nuclear matter EoS with increasing coupling strength [9]. The effective Lagrangian can be split into a free particle and an interaction part. The free part reads as

$$\mathcal{L}_{\rm kin} = \bar{q}\left(-i\gamma_\mu\partial_\mu + \hat{m} + \hat{\mu}\right) q\,, \tag{1}$$

where $\hat{m} = \mathrm{diag}(m_u, m_d, m_s)$ is the diagonal current quark mass matrix and $\hat{\mu}$ the corresponding quark chemical potential matrix. The effective interaction is written as

$$\begin{aligned}\mathcal{L}_{\rm int} \;=\; & G_{\rm S}\eta_{\rm D}\sum_{a,b=2,5,7}\left(\bar{q}i\gamma_5\tau_a\lambda_b C\bar{q}^T\right)\left(q^T C i\gamma_5\tau_a\lambda_a q\right)\\ & + G_{\rm S}\sum_{a=0}^{8}\left[(\bar{q}\tau_a q)^2 + \eta_{\rm V}(\bar{q}i\gamma_0 q)^2\right]\,.\end{aligned} \tag{2}$$

τ_a and λ_a are Gell-Mann matrices in flavor and color space respectively, and C the charge conjugation matrix. Here we have omitted interaction channels which do not contribute to the thermodynamics at meanfield level, like the pseudosclar isovector channel which would be required to make the chiral symmetry of this interaction model manifest. The parameter $G_{\rm S}$ defines the scalar coupling strength and can be determined from meson properties in the vacuum. For this study, we apply the parameters obtained for a sharp cut-off regularization scheme from Table III of Ref. [35] labeled with '∞' in front

of the corresponding table row[1]. The parameters $\eta_{\rm D}(\eta_{\rm V})$ are defined as the ratio of the diquark(vector) and scalar coupling. Since these two parameters are not fixed by vacuum properties of mesons or hadrons we treat them as free model parameters. In order to investigate thermodynamical properties of the system, we use the partition function in path integral representation

$$Z(T,\hat{\mu}) = \int \mathcal{D}\bar{q}\mathcal{D}q \exp\left\{\int_0^\beta d\tau \int d^3x \left[\bar{q}\left(i\partial\!\!\!/ - \hat{m} + \hat{\mu}\gamma^0\right) q + \mathcal{L}_{\rm int}\right]\right\} . \quad (3)$$

Bosonic meson field degrees of freedom can easily be introduced by applying corresponding Hubbard–Stratonovich transformations in all interaction channels. For the sake of simplicity, all of them are treated on the mean-field level, *viz.*, mesonic fluctuations and higher correlations are neglected. Minimizing the thermodynamical potential $\Omega = -T \ln Z$ with respect to the meanfields then defines the pressure $p = -\Omega$ of the equilibrated system. As a result of the minimization procedure one obtains a set of coupled gap equations which has to be solved selfconsistently. Finally, the thermodynamical potential reads as

$$\begin{aligned}\Omega(T,\mu) \;=\; & \frac{\phi_u^2+\phi_d^2+\phi_s^2}{8G_{\rm S}} - \frac{\omega_u^2+\omega_d^2+\omega_s^2}{8G_{\rm V}} + \frac{\Delta_{ud}^2+\Delta_{us}^2+\Delta_{ds}^2}{4G_{\rm D}} \\ & - \int \frac{d^3p}{(2\pi)^3} \sum_{n=1}^{18} \left[E_n + 2T \ln\left(1+e^{-E_n/T}\right)\right] + \Omega_l - \Omega_0 . \quad (4)\end{aligned}$$

Ω_l denotes the contribution of electrons and muons to the thermodynamic potential, Ω_0 is the contribution to be subtracted in order to obtain zero vacuum pressure. The ϕ_f (with $f = u,d,s$) are the chiral condensates corresponding to the three quark flavors which are obtained from the previously described minimization of the scalar meanfield terms. Accordingly, one has to account for the vector meanfields ω_f and pairing gaps $\Delta_{ff'}$. Under neutron star conditions, one additionally imposes electric charge neutrality and β-equilibrium conditions. In this paper, we disregard the Kobayashi–Maskawa–'t Hooft term in the interaction Lagrangian, see Ref. [33] for a motivation. Further references and possible consequences arising from the inclusion of this term are discussed in [36,37].

With Eq. (4) we have a QM EoS available which is still, by construction, phenomenological but allows to interpret the influence of certain interaction channels on the EoS more specifically than generalized power expansions of

[1] This parametrization scheme has been implemented in an online tool developed by F. Sandin which also corrects for a mistake in the kaon mass formula employed in [35], see `http://3fcs.pendicular.net/psolver`

ideal gas expressions. The next step, in order to describe NS phenomenology, is to account for confined nuclear matter at lower densities. Without a unified in-medium-approach for the description of nuclear matter in terms of QM degrees of freedom at hand we, as everybody else, fall back to a two-phase description, joining independently obtained nuclear and QM EoS by performing a phase transition construction. As common as this procedure is, we feel a few comments have to be made about it in order to avoid a misleading interpretation of this work. Our understanding of the nuclear EoS at supersaturation densities is by no means more profound than our knowledge about dense QM. The set of constraints we apply in order to pin down the QM EoS we originally bundled up in order to constrain the nuclear EoS. There are no profound additional insights into the shape of the 'true' nuclear matter EoS since the publication of [2]. even though progress has been made in order to gain deeper insights into the physics of finite density nuclear systems, *e.g.*, within the framework of chiral effective field theory [38] and directly from QCD via lattice simulations [39]. While these studies are progressing and may become applicable to high density nuclear systems in compact stars and heavy-ion collisions in future, we discuss these systems for the time being from the point of view of parametric approaches to the high density EoS. Such cold dense EoS studies may be guided by observations of compact stars, see [2, 40, 41]. From this parametric point of view the variation of model parameters of a QM EoS in a strict sense would always require to perform a similar variation of an independently obtained NM EoS. All results of this (or any similar) analysis, are likely to change significantly if the NM EoS is exchanged by a model with significantly different high density behavior. As an example, softening the NM EoS to a degree, where the model is not any longer in agreement with the two-solar mass, constraint requires to soften the QM EoS as well in order to obtain a thermodynamically sound phase transition. This makes it hard, if not impossible, to obtain a hybrid EoS which would describe a two solar mass NS. Still the QM EoS by itself is not necessarily in contradiction with the existence of high neutron star masses.

For our analysis, we avoid the problem of a nuclear parameter scan by applying the Dirac–Brueckner Hartree–Fock (DBHF) EoS which has proven to perform reasonably well for describing nuclear matter saturation properties and kaon data [42] as well as NS properties [2] even though it tends to behave too stiff above densities of about 3.5 times saturation density. On the other hand, this stiffness occurs in a region, where QM degrees of freedom are not unlikely to be the only ones which are relevant. Amongst other reasons we prefer the DBHF EoS because it is based on a relativistic and microscopical description of many-particle interactions. It starts from a given free nucleon–nucleon interaction (the relativistic Bonn A potential) fitted to nucleon–nucleon scattering data and deuteron properties. In *ab ini-*

tio calculations based on many-body techniques one then derives the nuclear energy functional from first principles, *i.e.*, treating short-range and many-body correlations explicitly. In the relativistic DBHF approach, the nucleon inside the medium is dressed by the self-energy based on a T-matrix. The in-medium T-matrix as obtained from the Bethe–Salpeter equation plays the role of an effective two-body interaction which contains all short-range and many-body correlations in the ladder approximation. As we have shown in the context of hybrid EoS the rather stiff behavior at high densities is not necessarily relevant if the phase transition to QM occurs at low enough densities of about three to four times saturation density [9].

3. Results

3.1. Hybrid neutron stars

Unlike to previous work, where we applied both, the flow and two-solar mass constraint, simultaneously in order to obtain a phenomenologically sound hybrid EoS [9] we start this analysis from calculating neutron star configurations for a wide range of vector and diquark couplings ($\eta_{\mathrm{V}} \in [0.0, 0.7]$, $\eta_{\mathrm{D}} \in [0.8, 1.15]$). To further extend the previous study we apply a different parameterization for the scalar coupling strength, as well, applying the parameters from the row labeled '∞' in Table I of Ref. [35]. As we will show, this choice significantly affects the outcome of the present study.

Before we discuss the overall result of a full variation of the two free parameters η_{V} and η_{D}, we keep one of them fixed at a reasonable value and vary the other. We consider any choice to be reasonable which eventually describes a two solar mass NS if one varies the one remaining free parameter. In Fig. 1 the vector coupling is kept constant at a value of $\eta_{\mathrm{V}} = 0.3$ while the diquark coupling is varied in the range $\eta_{\mathrm{D}} = 0.80 \ldots 1.10$. At 'low' values of η_{D}, here up to $\eta_{\mathrm{D}} = 1.00$, we find the required massive NS configurations. As one observes, an increase of η_{D} does not only result in a decrease of the maximum NS mass but lowers the critical density for the phase transition, too. In other words, an increase of η_{D} increases the content of QM in massive NS and lowers the maximum NS mass at the same time. On the other hand, keeping the diquark coupling η_{D} at a constant value and increasing the vector coupling will increase both, the maximum NS mass and the critical density. This is illustrated in Fig. 2. Again, there is a critical value of η_{V} corresponding to a minimal stiffness of the EoS which has to be exceeded in order to obtain NS configurations with a sufficiently high maximum mass. In the illustrated example for $\eta_{\mathrm{D}} = 1.0$ this holds for values larger than a critical coupling slightly above $\eta_{\mathrm{D}} = 0.2$.

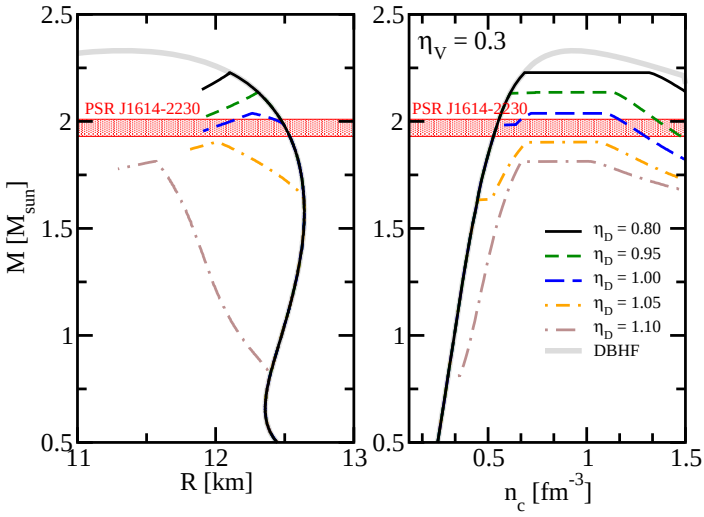

Fig. 1. At constant vector coupling (here $\eta_{\mathrm{V}} = 0.3$) an increase of η_{D} lowers both, the critical density and the maximum NS mass.

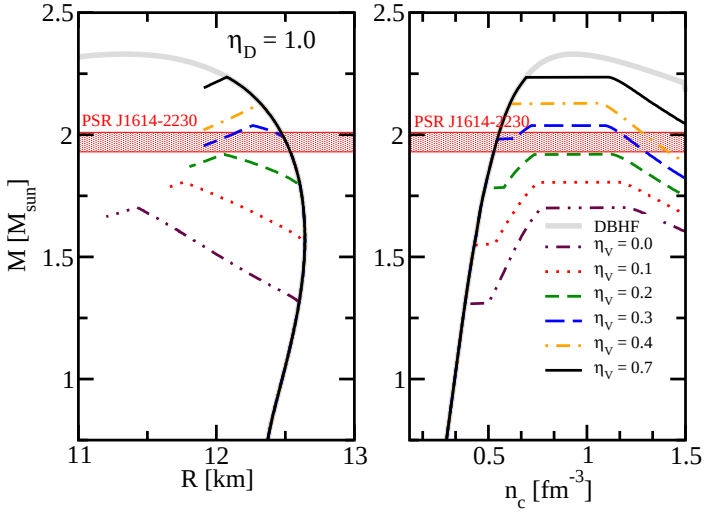

Fig. 2. At constant diquark coupling (here, $\eta_{\mathrm{D}} = 1.0$) an increase of η_{V} increases the maximum NS mass and the critical density.

With this understanding of the influence of η_{D} and η_{V} on both, the maximum NS mass and the critical density for the onset of the phase transition we now perform a variation over the full available parameter space region of η_{D}–η_{V} in which we can obtain stable hybrid NS configurations.

The result of this study is summarized in Fig. 3, which we will now discuss in detail. From the obtained mass-radius and mass-density relations of each of the differently parameterized hybrid EoS we extracted two numbers only, the maximum possible NS mass and the NS mass at which the central density becomes large enough to generate a QM core in the NS. Consequently, we call the latter quantity M_{onset}. The middle gray (red) band in Fig. 3 labeled PSR J1614-2230 corresponds to EoS parameterizations which describe a maximum mass exactly within the interval $M = 1.97 \pm 0.04\, M_{\odot}$ as it has been reported for PSR J1614-2230. As we understand from the previous paragraphs, it is possible to obtain more massive solutions by increasing η_{V} or decreasing η_{D}. As both of these operations increase the transition density, one eventually obtains massive NS which are purely hadronic. This can be either because the transition occurs at very large densities which are not realized in NS or, more relevant for our considerations, because the hybrid NS solutions become unstable. Examples for this situation are found in Fig. 2 for all $\eta_{\mathrm{V}} > 0.4$. The hatched upper left/cyan region in Fig. 3 corresponds to all EoS parameterizations which result in unstable hybrid solutions. The opposite extreme scenario results from increasing η_{D} or decreasing η_{V}. Then, the transition density is lowered until eventually

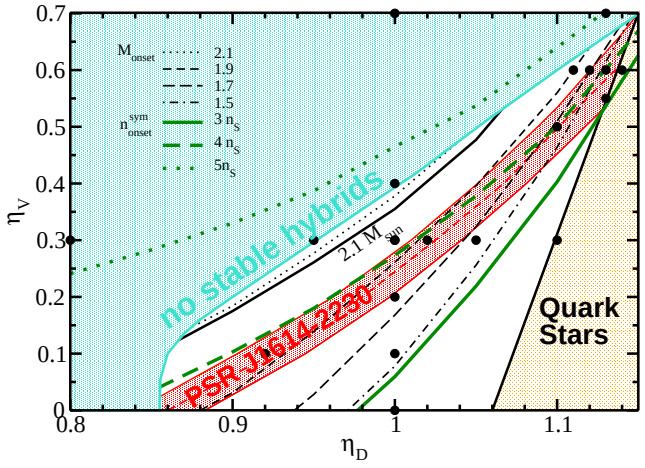

Fig. 3. The overall result of the parameter study of the NJL model concerning the vector (η_{V}) and diquark (η_{D}) channel coupling. The middle gray (red) band and all parameter pairs over it correspond to EoS which reproduce at least $1.97 \pm 0.04\, M_{\odot}$ (PSR J1614-2230), in the upper left gray (cyan) region no stable hybrid configurations are found, while the right gray region corresponds to 'mostly' quark stars. A more detailed discussion is given in the text. Black filled circles correspond to parameterizations mentioned in the text.

only a thin hadronic layer remains and the NS are basically pure quark star configurations. This scenario corresponds to the gray (orange) region labeled 'Quark Stars'. In this parameter region, the quark matter EoS has an early onset of the pressure due to a decrease of the dynamical quark mass before the first order phase transition which results in a low QM transition density.

It is interesting to observe that there is a band (middle gray (red)) of EoS parameters in the η_D–η_V plane with resulting maximum NS masses of $1.97 \pm 0.04\, M_\odot$. While the middle gray (red) band in Fig. 3 denotes configurations with *maximum* masses corresponding to PSR J1614, it is worthwhile to ask for the actual quark content of these configurations. For the purpose of this article we will make a qualitative statement, only, and postpone quantitative analyses to a later publication. The curves labeled $M_{\rm onset}$ in Fig. 3 indicate from which NS mass on the EoS results in hybrid NS solutions. Hence it is favorable to have a small value of $M_{\rm onset}$ in order to obtain large QM cores. Therefore, the largest QM content for a high mass NS has to be expected in the upper right corner of Fig. 3. This is illustrated in Fig. 4. We point out that the middle gray (red) band describes NS configurations, where the maximum mass corresponds to the reported mass of PSR J1614, only. Of course, more massive NS are possible. As we are interested in massive NS with large quark cores, Fig. 5 shows NS configurations from the upper right corner of Fig. 3. Large quark cores in our EoS parameterization are in general favored for values of $\eta_V = 0.5 \ldots 0.6$. This is in vicinity of

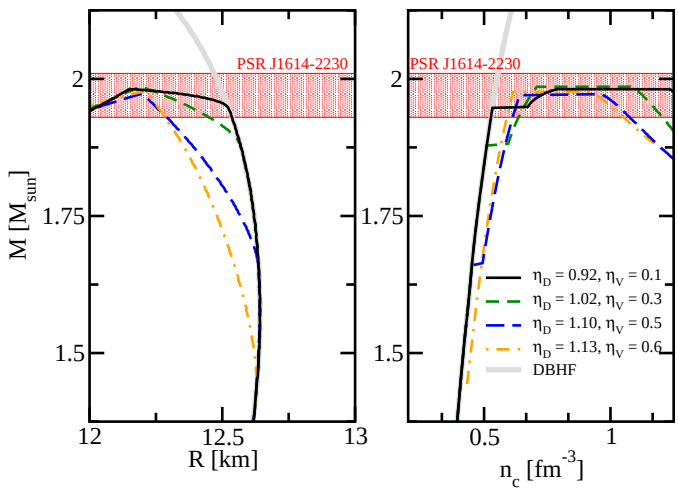

Fig. 4. Systematics of mass-radius and mass-central density curves for chosen parameter sets with maximum mass equal to that of PSR J1614-2230. Large values of η_D and η_V result in a phase transition at lower densities and, therefore, a higher content of QM for massive NS.

the value $\eta_{\rm V}^{\rm F} = 0.5$ as obtained after Fierz transformation of the one-gluon exchange interaction (details in Ref. [18]). It is noteworthy, that comparable small changes of the diquark coupling constant strongly affect the transition density. As an example, Fig. 5 illustrates that with constant $\eta_{\rm V} = 0.6$ a change of a few percent in $\eta_{\rm D}$ ($= 1.11 \ldots 1.14$) makes the difference whether a rather typical NS with a mass of, *e.g.*, $M = 1.4\, M_\odot$ has QM content or not.

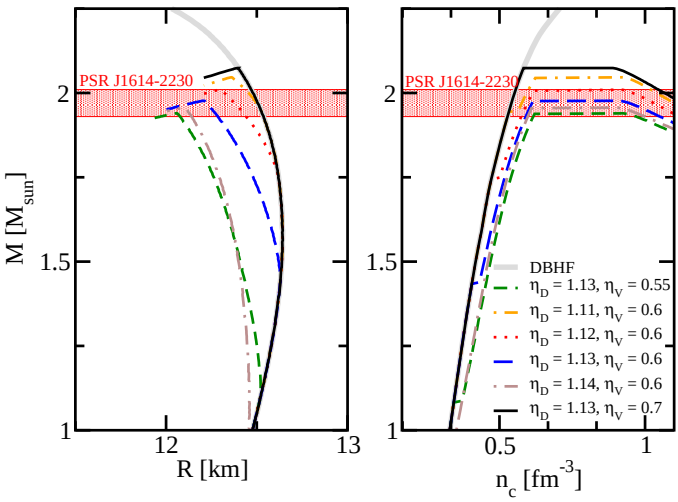

Fig. 5. Mass-radius and mass-central density relation for a selection of EoS parameterizations with mostly significant QM core (as found in the upper right corner of Fig. 3).

3.2. Implications for HIC

In isospin-symmetric matter as found in HIC our main statements regarding the influence of $\eta_{\rm V}$ and $\eta_{\rm D}$ on the stiffness of the EoS and the transition density do not change. Increasing $\eta_{\rm V}$ at constant $\eta_{\rm D}$ increases the stiffness and the transition density, increasing $\eta_{\rm D}$ at constant $\eta_{\rm V}$ reduces the stiffness and lowers the transition density. The transition densities in symmetric matter are plotted in Fig. 3, labeled as $n_{\rm onset}^{\rm sym}$. It is remarkable that along the middle gray (red) band (configurations with maximum masses corresponding to the mass of PSR J1614) the transition density in symmetric matter has an almost constant value of $n_{\rm onset}^{\rm sym} \approx 4 n_{\rm S}$. This is a distinct difference to what we learned for the electrically neutral and β-equilibrated EoS for NS matter, where the transition density decreased from the lower left to the upper right within the middle gray (red) band. Since the transition density in symmetric matter is lower only below the middle gray (red)

band, a region where the maximum NS masses are not sufficiently large this model predicts $n_{\rm onset}^{\rm sym} \approx 4n_{\rm S}$ as a lower limit on the critical density for the phase transition in symmetric matter. It is necessary to point out, that our previous study [9] gave a different result and predicted a lower transition density. In order to illustrate this, we plot hybrid EoS parameterizations in symmetric matter corresponding to NS EoS with maximum masses of $1.97 \pm 0.04\,M_\odot$ (along the middle gray (red) band in Fig. 3) in Fig. 6 and our previous result in Fig. 7. While Fig. 6 suggests, that the phase transition occurs at densities too high to prevent the nuclear DBHF EoS from violating the flow constraint, our old results in Fig. 7 perform significantly better. This observation gives our study a surprising twist which we will investigate in future work. The reason for this different behavior is not hard to comprehend. Both EoS start from a different parameterization already on the level of the scalar coupling constant. The larger dynamical quark mass resulting from the parameterization applied for the present study (see [35] for the actual values) causes a general shift of the QM onset to larger chemical potentials. Therefore, the phase transition from nuclear to QM simply follows this trend. From our perspective, this is the first time, that high density observables as elliptic flow and maximum NS masses can actually be applied to distinguish models with different parameterizations in the scalar channel. Of course, the usual caveats have to be made, lead by the most serious one: In order to draw final conclusions, first it has to be made clear beyond any doubt, that NS actually have a QM core. At the current stage, this statement is neither proven nor disproven. If observational evidence in favor of the presence of QM in NS should ever arise, many more statements

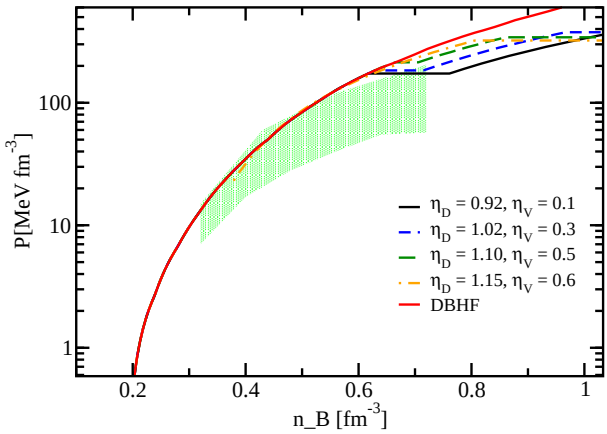

Fig. 6. Flow constraint of symmetric equation of state for chosen parameter sets with maximum masses equal to that of PSR J1614-2230.

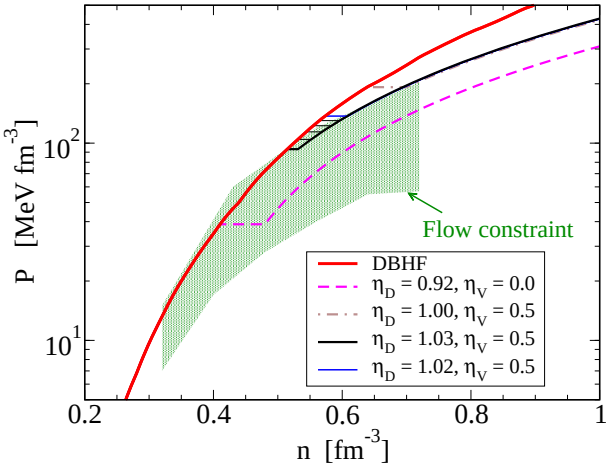

Fig. 7. In previous work [9] better agreement with the flow constraint has been achieved. Reason is a different parameterization which in particular results in a smaller dynamical quark mass in vacuum.

can be made, not only about the transition density in symmetric matter. Large NS masses require rather stiff QM EoS. As a consequence, the transition region in the density domain is not very large. This is illustrated in Table I by a few examples for parameters within the middle gray (red) band in Fig. 3 by calculating the difference Δn between QM and NM density at the phase transition. Since the quark content increases with η_V a clear signature for QM in NS would imply at least $\Delta n < n_S \approx 0.16$ fm^{-3}.

TABLE I

Density difference between QM and NM at the phase transition for a few parameterizations with $M_{\max} \in (1.97 \pm 0.04)\, M_\odot$.

η_V	0.1	0.2	0.3	0.5	0.6
η_D	0.92	0.98	1.02	1.10	1.15
Δn [fm^{-3}]	0.144	0.107	0.086	0.041	0.017

4. Conclusions

We performed a systematic model analysis of an NJL-type EoS, where we investigated the dependence of NS properties on the diquark and vector coupling constants. It is possible to describe NS configurations with a significant amount of QM and maximum NS masses which are in agreement with the reported high mass of PSR J1614-2230. The amount of QM in an NS will increase with increasing vector coupling if the diquark coupling is adjusted

accordingly. Therefore, both channels are important for the understanding of NS phenomenology. Due to a different choice of the scalar coupling and the resulting larger dynamical quark mass, the present model parameterization does not resolve the conflict of the nuclear DBHF EoS with the flow constraint. This result is of great importance since it implies that without a sound understanding of the chiral phase transition in medium, otherwise identical, models can come to quantitatively significantly different results. In particular, this raises doubts about the predictive power of any EoS which does not account for the mechanism of chiral symmetry breaking. Of course, we do not intend to imply, that NJL-type models will provide the ultimate tool to describe the QCD-phase transition qualitatively and quantitatively correct. There are many open questions, which will need to be addressed in the future, most importantly the mechanism of confinement/deconfinement in medium. Significant improvement of any existing model is required in order to understand this phenomenon and to finally get rid of the necessity to construct thermodynamically motivated Maxwell- and Gibbs-phase transitions, which are not suited to provide deeper insights into the microphysical mechanisms governing QCD phase transformations. First steps in this direction have been performed within a generalized NJL model [43]. Further progress was made in a microscopic description of the baryon dissociation in dense matter, based again on a NJL model approach [44], where, in particular, the interplay between chiral symmetry restoration and diquark condensation transitions at high densities for the spectral function of nucleons has been investigated. Further steps will be taken towards the development of an EoS which describes the Mott dissociation of baryons into their quark constituents in a consistent way which accounts for nucleonic bound and scattering states simultaneously. An EoS of this quality has been developed within a generalized Bethe–Uhlenbeck approach for strongly interacting matter in order to describe the Mott dissociation of deuterons in nuclear matter [45] (see also recent work on cluster formation in low-density nuclear matter [46, 47]) and the Mott effect for mesons in quark matter [48, 49].

The authors acknowledge valuable discussions and collaboration, in particular, with J. Berdermann, M. Buballa, H. Grigorian, G. Poghosyan, C.D. Roberts, G. Röpke, S. Typel, D.N. Voskresensky, F. Weber, H. Wolter and D. Zablocki. This work has been supported in part by "CompStar", a Research Networking Programme of the European Science Foundation and by the Polish Ministry for Science and Higher Education under grant No. NN 202 2318 37. The work of D.B. has been supported by the Russian Fund for Fundamental Investigations under grant No. 11-02-01538-a. T.K. is supported by the network "hadronphysics3" within the seventh framework programme of the European Union.

REFERENCES

[1] J.M. Lattimer, M. Prakash, arXiv:1012.3208 [astro-ph.SR].

[2] T. Klähn *et al.*, *Phys. Rev.* **C74**, 035802 (2006).

[3] J.M. Lattimer, M. Prakash, *Phys. Rep.* **442**, 109 (2007).

[4] P. Demorest *et al.*, *Nature* **467**, 1081 (2010).

[5] I. Bednarek, R. Manka, *J. Phys. G* **36**, 095201 (2009).

[6] M. Bejger, J.L. Zdunik, P. Haensel, M. Fortin, *Astron. Astrophys.* **536**, A92 (2011) [arXiv:1109.1179 [astro-ph.HE]].

[7] J. Rikovska-Stone, P.A.M. Guichon, H.H. Matevosyan, A.W. Thomas, *Nucl. Phys.* **A792**, 341 (2007).

[8] J.R. Stone, P.A.M. Guichon, A.W. Thomas, arXiv:1012.2919 [nucl-th].

[9] T. Klähn *et al.*, *Phys. Lett.* **B654**, 170 (2007).

[10] D.J. Nice, I.H. Stairs, L. Kasian, *Bull. Am. Astron. Soc.* **39**, 918 (2007).

[11] P. Danielewicz, R. Lacey, W.G. Lynch, *Science* **298**, 1592 (2002).

[12] Y. Nambu, G. Jona-Lasinio, *Phys. Rev.* **122**, 345 (1961).

[13] Y. Nambu, G. Jona-Lasinio, *Phys. Rev.* **124**, 246 (1961).

[14] M.K. Volkov, *Sov. J. Part. Nucl.* **17**, 186 (1986) [*Fiz. Elem. Chast. Atom. Yadra* **17**, 433 (1986)].

[15] U. Vogl, W. Weise, *Prog. Part. Nucl. Phys.* **27**, 195 (1991).

[16] S.P. Klevansky, *Rev. Mod. Phys.* **64**, 649 (1992).

[17] T. Hatsuda, T. Kunihiro, *Phys. Rep.* **247**, 221 (1994).

[18] M. Buballa, *Phys. Rep.* **407**, 205 (2005).

[19] F. Özel *et al.*, *Astrophys. J.* **724**, L199 (2010).

[20] S. Weissenborn *et al.*, *Astrophys. J.* **740**, L14 (2011).

[21] M. Alford, M. Braby, M.W. Paris, S. Reddy, *Astrophys. J.* **629**, 969 (2005).

[22] T. Klähn *et al.*, *Phys. Rev.* **C82**, 035801 (2010).

[23] D. Blaschke, H. Grigorian, A. Khalatyan, D.N. Voskresensky, *Nucl. Phys. Proc. Suppl.* **141**, 137 (2005).

[24] A.E. Radzhabov, D. Blaschke, M. Buballa, M.K. Volkov, *Phys. Rev.* **D83**, 116004 (2011).

[25] D. Horvatic, D. Blaschke, D. Klabucar, O. Kaczmarek, *Phys. Rev.* **D84**, 016005 (2011).

[26] D.B. Blaschke *et al.*, *Phys. Rev.* **C75**, 065804 (2007).

[27] A.G. Grunfeld *et al.*, *Int. J. Mod. Phys.* **E16**, 2842 (2007).

[28] S. Noguera, N.N. Scoccola, *Phys. Rev.* **D78**, 114002 (2008).

[29] T. Hell, S. Roessner, M. Cristoforetti, W. Weise, *Phys. Rev.* **D79**, 014022 (2009).

[30] T. Hell, K. Kashiwa, W. Weise, *Phys. Rev.* **D83**, 114008 (2011).

[31] G.A. Contrera, M. Orsaria, N.N. Scoccola, *Phys. Rev.* **D82**, 054026 (2010).

[32] S.B. Ruester *et al.*, *Phys. Rev.* **D72**, 034004 (2005).
[33] D. Blaschke *et al.*, *Phys. Rev.* **D72**, 065020 (2005).
[34] H. Abuki, T. Kunihiro, *Nucl. Phys.* **A768**, 118 (2006).
[35] H. Grigorian, *Phys. Part. Nucl. Lett.* **4**, 223 (2007).
[36] D. Blaschke, J. Berdermann, R. Lastowiecki, *Prog. Theor. Phys. Suppl.* **186**, 81 (2010).
[37] D. Blaschke, T. Klähn, R. Lastowiecki, F. Sandin, *J. Phys. G* **37**, 094063 (2010).
[38] A. Lacour, J.A. Oller, U.G. Meissner, *Ann. Phys.* **326**, 241 (2011).
[39] T. Hatsuda, `arXiv:1101.1463 [nucl-th]`.
[40] F. Özel, G. Baym, T. Guver, *Phys. Rev.* **D82**, 101301 (2010).
[41] A.W. Steiner, J.M. Lattimer, E.F. Brown, *Astrophys. J.* **722**, 33 (2010).
[42] C. Fuchs, *Lect. Notes Phys.* **641**, 119 (2004).
[43] S. Lawley, W. Bentz, A.W. Thomas, *J. Phys. G* **32**, 667 (2006).
[44] J.-C. Wang, Q. Wang, D.H. Rischke, *Phys. Lett.* **B704**, 347 (2011).
[45] M. Schmidt, G. Röpke, H. Schulz, *Ann. Phys.* **202**, 57 (1990).
[46] S. Typel *et al.*, *Phys. Rev.* **C81**, 015803 (2010).
[47] M. Hempel, J. Schaffner-Bielich, S. Typel, G. Röpke, *Phys. Rev.* **C84**, 055804 (2011) [`arXiv:1109.0252 [nucl-th]`].
[48] J. Hüfner, S.P. Klevansky, P. Zhuang, H. Voss, *Ann. Phys.* **234**, 225 (1994).
[49] P. Zhuang, J. Hüfner, S.P. Klevansky, *Nucl. Phys.* **A576**, 525 (1994).